SHORT COMMUNICATION

Effect of nanoclay content on properties of glass–waterborne epoxy laminates at low clay loading

L. Aktas and M. C. Altan*

The effect of nanoclay content on the properties of glass fibre reinforced, waterborne epoxy laminates is investigated. Fourteen ply nanocomposite laminates containing 0, 0·1, 0·2, 0·5, 1 and 2 wt-% cloisite Na^+ nanoclay are fabricated by a hot press. The interlaminar shear strength, flexural strength and flexural stiffness of the fabricated nanocomposites are characterised. In addition, the thermal stability of the laminates is investigated using thermogravimetric analysis; the state of dispersion is studied by X-ray diffraction, and the fibre–matrix adhesion is assessed using scanning electron microscopy on fracture surfaces. Mechanical properties peaked at a nanoclay loading of 0·5 wt-%. At this low nanoclay loading, the improvements in interlaminar shear strength, flexural strength and flexural stiffness were 5, 8 and 12% respectively. Thermogravimetric analysis indicated moderate improvements in thermal stability. X-ray diffraction, on the other hand, indicated complete exfoliation of nanoclay platelets for 0·1, 0·2 and 0·5 wt-% loadings. A subtle peak appeared for nanoclay loadings of 1 and 2 wt-% at a gallery spacing of 17 Å. Scanning electron micrographs indicated improved fibre–matrix adhesion with increasing nanoclay content as evidenced by increased amount of matrix residues on the fibre bundles after fracture.

Keywords: Nanocomposites, Low nanoclay content, Waterborne epoxy

Introduction

Various properties of nanoclay reinforced polymers have been studied following their first introduction more than a decade ago.[1–3] Majority of these studies dealt with the mechanical property improvements in thermoplastics and thermosetting polymers due to the addition of nanoclay up to 10 wt-%. When nanoclay is mixed with thermoplastics and rubbery thermosets, mechanical properties are frequently improved. For instance, improvements up to 54% in stiffness and 15% in yield strength of thermoplastic polyolefins were reported.[4] Similar improvements were also observed in polypropylene and polyethylene systems.[5,6] In addition to mechanical properties, nanoclay was observed to alter the crystal structure of thermoplastics. As reported by Yuan *et al.*[7,8], nanoclay platelets act as crystal nucleation sites in polypropylene and polyethylene.

However, in higher performance glassy thermosets, the improvements in mechanical properties remain marginal.[9,10] The marginal improvement (or deterioration) in mechanical properties of glassy thermosets is often associated with agglomeration or incomplete exfoliation of the nanoclay platelets.[11–13] Compared with thermoplastics and rubbery thermosets, complete dispersion and separation of clay platelets are particularly important in stronger glassy polymers or their fibre reinforced composites.

Several mechanical and chemical techniques, including different nanoclay surface modification methods, have been tried to facilitate total separation of individual platelets (i.e. exfoliation) in a polymeric matrix. However, above a certain concentration level, the physical space available for the peel-off and separation of high aspect ratio of clay platelets will be severely limited, thus preventing effective exfoliation and load transfer. To benefit from the nanoscale properties of clay and achieve effective load transfer between the matrix and clay platelets, each platelet needs to have adequate physical space to rotate and peel off from a larger clay stack or cluster.

Estimating average spacing between clay platelets for a given concentration level and platelet aspect ratio is rather straightforward. If the average spacing between clay platelets in a suspension is as large as the platelet's planar dimension, then each platelet will, on average, have adequate volume in the suspension to rotate freely without being hindered by the neighbouring platelets. This volume fraction level Φ_v is usually referred to as the dilute regime and can be calculated for a thin, disc shaped nanoclay platelet of diameter d and thickness t as

School of Aerospace and Mechanical Engineering, University of Oklahoma, Room 212, 865 Asp Avenue, Norman, OK 73072, USA

*Corresponding author, email altan@ou.edu

Published by Maney on behalf of the Institute
Received 3 February 2009; accepted 24 February 2009
DOI 10.1179/174328409X428864

$$\Phi_v = \frac{\pi d^2 t/4}{(4/3)\pi(d/2)^3} = 1{\cdot}5(d/t)^{-1} \quad (1)$$

where d/t is the aspect ratio of a nanoclay platelet. Equation (1) can be used to determine the volume fraction of the clay loading above which the motion of a platelet will be influenced and physically restricted by its neighbours. Thus, it would be unrealistic to expect full exfoliation of platelets at volume fractions much higher than the value estimated by equation (1), as platelets will not have adequate space to separate and rotate during processing.

The thickness of a nanoclay platelet has been well documented by molecular studies as $\sim$1 nm.[14,15] Transmission electron microscopy and atomic force microscopy analyses indicate that the surface dimension of a nanoclay platelet ranges from 600 up to 800 nm.[16] Planar surface dimensions as small as 200 nm have also been reported by Fornes and Paul.[17] It can be seen from equation (1) that, to prevent interaction of nanoclay platelets with each other and to fully exfoliate platelet stacks, the nanoclay volume fraction of the matrix phase needs to be less than 0·75% for an aspect ratio of 200 and even less than 0·1875% for 800. Such low volume fraction levels would translate to a weight fraction range of 0·3–1 wt-%, depending on the densities of clay and resin used. In the present study, final nanoclay contents of 0, 0·1, 0·2, 0·5, 1 and 2 wt-% are chosen to determine the effect of low nanoclay content on the mechanical properties of glass fibre reinforced waterborne epoxy laminates. It is expected that, for this waterborne epoxy system, clay weight fraction as low as 0·5% would facilitate effective dispersion in an aqueous medium and thus improve mechanical properties of the laminate.

Experimental

The waterborne epoxy resin used for the current study is EpiRez 3522-w-60 from Hexion Chemicals. As recommended by the materials supplier, 0·15 parts of 2-methylimidazole and 1·2 parts of dicyandiamide dispersed in 21 parts of distilled water at 70°C are used as the cure agent. Before mixing with 100 parts of waterborne epoxy resin, desired amounts of nanoclay (Cloisite Na^+) is added to the aqueous cure agent dispersion.

The waterborne epoxy resin, cure agent and nanoclay mixture are used to prepare prepregs by wetting 152·4 × 228·6 mm chopped strand glass fibre preforms and squeezing out the excess resin by a stainless steel roller. These wet preforms are then placed into a convective oven at 120°C for 20 min allowing water to evaporate and obtain dry, non-tacky prepregs ready for laminate fabrication. Fourteen layers of 76·2 × 76·2 mm prepregs are cut out from these larger sheets and stacked together for the fabrication of a single laminate. The glass fibre content of each laminate is determined to be 47 wt-%.

A total of 18 laminates (three for each nanoclay content) with an average thickness of 3·2 mm are fabricated using a heated compression mould. The cure cycle involves two steps. First, the temperature is increased from room temperature to 65·5°C at a rate of 5°C min^{-1} and kept at that temperature for 10 min. The temperature where the viscosity of the system is the lowest is determined to be at 65·5°C. Following this initial hold, temperature is increased once more to 121·1°C at a rate of 5°C min^{-1}. The laminates are allowed to cure at that temperature for 30 min before cooling down to room temperature. For each nanoclay content, a total of 10 samples with dimensions 63·5 × 11 mm are prepared from the two laminates to be used in flexural testing. Flexural testing is carried out per ASTM D2344/D2344M-00 standard in three point bending configuration with a span of 57·15 mm. A total of 10 samples with dimensions 31·7 × 11 mm at a span of 25·4 mm are obtained from the remaining laminate to characterise the interlaminar shear strength (ISS).

Thermal stability of the samples is characterised by thermogravimetric analysis (TGA) using STA625 simultaneous thermal analyser by Rheometric Scientific Inc. Samples weighing at least 25 mg are placed in the TGA cell and continuously weighed while the temperature is ramped from ambient to 610°C at a rate of 10°C min^{-1}. The gallery spacing of Cloisite Na^+ is determined by wide angle X-ray diffraction (XRD). Samples for wide angle XRD are prepared by placing a small amount of clay between two layers of scotch tape. In addition, composite samples with a thickness of 100 μm are cut from the discs for small angle XRD to determine the change in gallery spacing of clay after fabrication of the composite parts. Fibre–matrix adhesion is characterised by SEM. Images of the fracture surfaces of tested samples and matrix residues on the fibre surfaces are studied at various magnifications ranging from × 500 to × 5000.

Results and discussion

Interlaminar shear strength of nanocomposite samples is shown in Fig. 1*A*, with error bars depicting 95% confidence intervals. It is observed that the ISS of the samples comprised of 0·1, 0·2 and 0·5 wt-% nanoclay are improved over the sample without nanoclay. The ISS reached its maximum at 0·5 wt-% loading with 5% improvement. In a previous study,[18] the ISS of a similarly fabricated nanocomposite monotonically decreased with the addition of 1, 2 and 4 wt-% nanoclay, thus agreeing with the current results. The increase in ISS at these relatively low nanoclay contents is most likely due to the exfoliation of the platelets facilitated by the reduced interaction of nanoclay platelets with each other.

Similar results are obtained for flexural strength and stiffness as shown in Fig. 1*B*. Both flexural strength and stiffness are observed to have their maximum at 0·5 wt-% nanoclay loading. For instance, flexural stiffness increased by 12% from 14·6 to 16·3 GPa at 0·5 wt-% nanoclay loading. Flexural strength, on the other hand, increased by 8% over the same range. When nanoclay content is increased above 0·5 wt-%, both flexural stiffness and strength are observed to deteriorate possibly due to stacking of high aspect ratio clay platelets with limited intercalation or exfoliation. Corroborating these results, an increase in both impact strength and tensile strength of moulded clay–epoxy composites without glass fibres was also reported for low nanoclay loadings of 1 wt-% or less.[19]

The TGA spectra of nanocomposite samples, as shown in Fig. 2, follow similar trends, except for the onset of thermal degradation. Increasing nanoclay

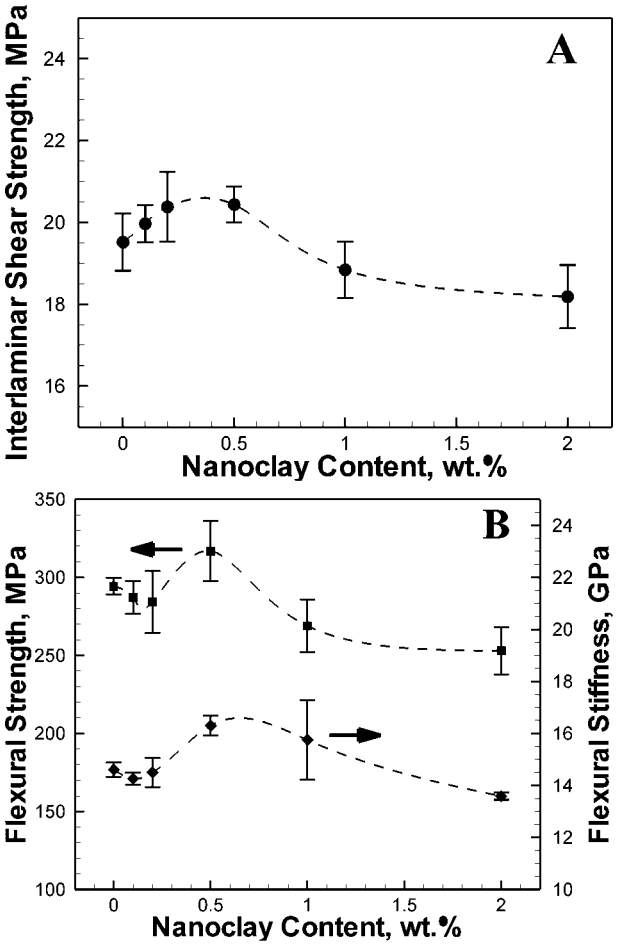

1 ***A*** **interlaminar shear strength of composite and nanocomposite samples and** ***B*** **flexural strength and stiffness of composite and nanocomposite samples**

content is observed to improve the temperature at which thermal degradation starts, which is also shown as an inset in Fig. 2. For example, as the temperature is increased to 400°C, composite sample without nanoclay loses 11% of its initial weight, whereas samples containing 0·5 and 2 wt-% nanoclay only lose 9·5 and 8·3% respectively. This behaviour confirms the reports that an outer char layer, formed due to the presence of nanoclay, delays the thermal degradation process for the part.[20]

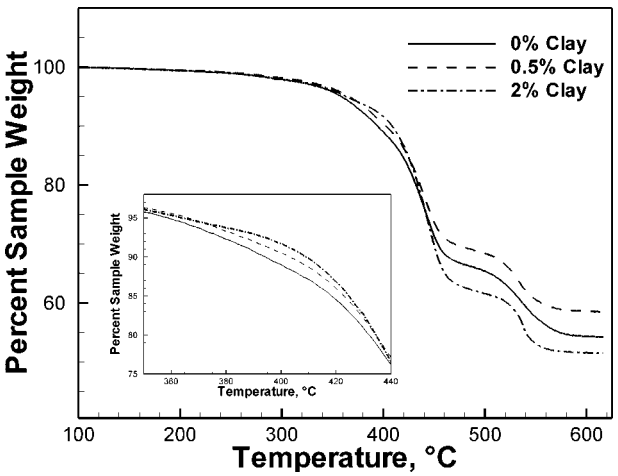

2 Thermogravimetric spectra of nanocomposites

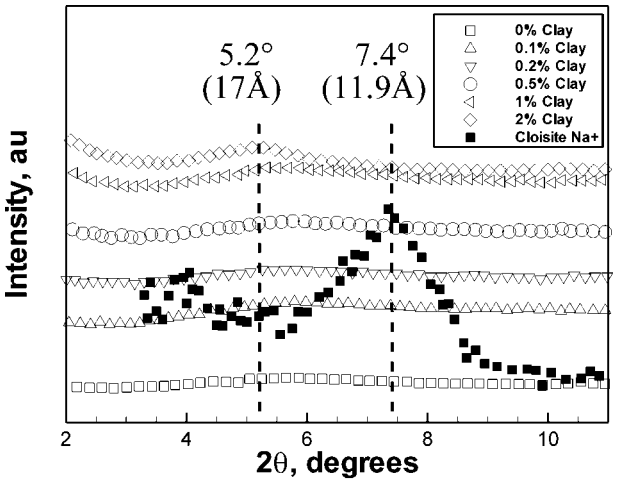

3 X-ray diffraction spectra of composite and nanocomposite samples and Cloisite Na^+ nanoclay

X-ray diffraction spectra of the nanocomposite samples and Cloisite Na^+ are shown in Fig. 3. The Cloisite Na^+ sample displayed a peak at 7·4° which, through Bragg's Law, corresponding to a gallery spacing of 11·9 Å under Cu K_α radiation. This gallery spacing is in agreement with the 11·7 Å value provided by the supplier. The nanocomposites containing 0·1, 0·2 and 0·5 wt-% nanoclay, on the other hand, did not display a peak, indicating effective dispersion of nanoclay. However, as the nanoclay content is increased to 1 and 2 wt-%, a subtle peak at 5·2° appears, suggesting a gallery spacing of 17 Å. The enlarged gallery spacing indicates intercalation of clay during processing, despite forming stacks detectable by the XRD. Owing to the limited physical space at 1 or 2 wt-% concentration, large aspect ratio clay platelets seem to form intercalated stacks or clusters, which lead to reduced mechanical performance.

The SEM images of the fracture surfaces of 0, 0·1 and 0·5 wt-% nanoclay are shown in Fig. 4. The microstructures of the samples containing nanoclay are notably different. Matrix residues that are observed on fibre bundles are unequivocal signs of effective fibre–matrix adhesion. It should also be noted that, for samples containing nanoclay, resin–clay residue around the fibres is significantly more than those samples without nanoclay. Increased resin–clay residue on the fibre surfaces indicates that the addition of nanoclay improved the fibre–matrix adhesion at low levels of clay concentration, which could partly contribute to the improved mechanical properties.

Conclusions

Nanocomposite laminates containing unmodified nanoclay (i.e. Cloisite Na^+) and randomly oriented chopped glass fibres are prepared using waterborne epoxy resin via compression moulding. The clay contents of the laminates are chosen as 0, 0·1, 0·2, 0·5, 1 and 2 wt-% to characterise the property changes at low levels of nanoclay loading.

It is observed that ISS, flexural strength and flexural stiffness yield their maximum values at 0·5 wt-% nanoclay loading, with 5, 8 and 12% improvement over the composite sample without nanoclay respectively. Thermogravimetric analysis showed moderate

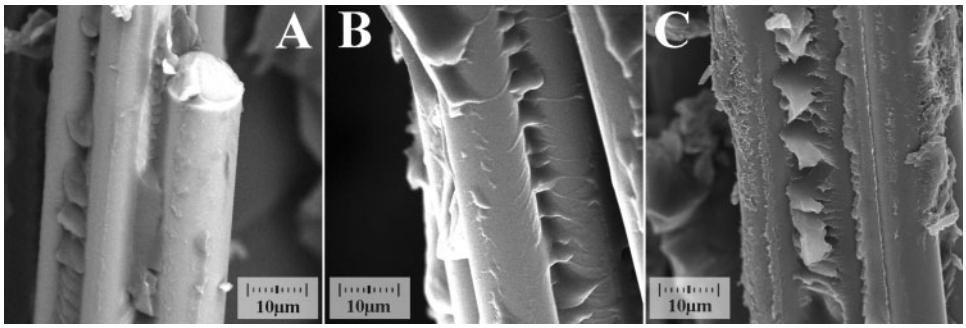

A composite without nanoclay; *B* nanocomposite with 0·1 wt-% nanoclay; *C* nanocomposite with 0·5 wt-% nanoclay

4 Scanning electron micrographs of fracture surfaces captured at ×1000

improvement in the temperature at which the thermal degradation started. X-ray diffraction analyses indicated complete exfoliation for samples containing 0·1, 0·2 and 0·5 wt-% nanoclay. However, as the nanoclay content increased to 1 and 2 wt-%, a subtle peak at 17 Å indicated the presence of intercalated stacks of clay platelets. Scanning electron microscopy images of the fracture surfaces revealed improved fibre matrix adhesion for samples containing nanoclay, as evidenced by the considerable amount of matrix residue on the fractured fibre bundles.

References

1. A. Usuki, M. Kawasumi, Y. Kojima, A. Okada, T. Kurauchi and O. Kamigaito: *J. Mater. Res.*, 1993, **8**, 1174–1178.
2. A. Usuki, Y. Kojima, M. Kawasumi, A. Okada, Y. Fukushima, T. Kurauchi and O. Kamigaito: *J. Mater. Res.*, 1993, **8**, 1179–1184.
3. Y. Kojima, A. Usuki, M. Kawasumi, A. Okada, Y. Fukushima, T. Kurauchi and O. Kamigaito: *J. Mater. Res.*, 1993, **8**, 1185–1189.
4. C. Deshmane, Q. Yuan and R. D. K. Misra: *Mater. Sci. Eng. A*, 2007, **A460**–**A461**, 277–287.
5. C. Deshmane, Q. Yuan, R. S. Perkins and R. D. K. Misra: *Mater. Sci. Eng. A*, 2007, **A458**, 150–157.
6. Q. Yuan and R. D. K. Misra: *Polymer*, 2006, **47**, 4421–4433.
7. Q. Yuan, S. Awate and R. D. K. Misra: *Eur. Polym. J.*, 2006, **42**, 1994–2003.
8. Q. Yuan, S. Awate and R. D. K. Misra: *J. Appl. Polym. Sci.*, 2006, **102**, 3809–3818.
9. T. Lan and T. J. Pinnavaia: *Chem. Mater.*, 1994, **6**, 2216–2219.
10. L. Aktas, Y. K. Hamidi and M. C. Altan: *J. Eng. Mater. Technol.*, 2008, **130**, 1–9.
11. J. L. Abot, A. Yasmin and I. M. Daniel: *Mater. Res. Soc. Symp. Proc.*, 2003, **740**, I6·5·1–I6·5·6.
12. L. Aktas, S. Dharmavaram, Y. K. Hamidi and M. C. Altan: *J. Compos. Mater.*, 2008, **21**, 2209–2229.
13. L. Aktas, Y. K. Hamidi and M. C. Altan: *Plast., Rubber Compos.*, 2004, **33**, 267–272.
14. H. J. Ploehn and C. Liu: *Ind. Eng. Chem. Res.*, 2006, **45**, 7025–7034.
15. S. J. Ahmadi, Y. D. Huang and W. Li: *J. Mater. Sci.*, 2004, **39**, 1919–1925.
16. H. Miyagawa, M. J. Rich and L. T. Drzal: *J. Polym. Sci. B, Polym. Phys.*, 2004, **42**, 4391–4400.
17. T. D. Fornes and D. R. Paul: *Polymer*, 2003, **44**, 4993–5013.
18. L. Aktas and M. C. Altan: *Polym. Compos.*, to be published.
19. C. Basara, U. Yilmazer and G. Bayram: *J. Appl. Polym. Sci.*, 2005, **98**, 1081–1086.
20. T. Kashiwagi, R. H. Harris, X. Zhang, R. M. Briber, B. H. Cipriano, S. R. Raghavan, W. H. Awad and J. R. Shields: *Polymer*, 2004, **45**, 881–891.